Near-infrared (NIR) diffuse reflectance spectroscopy for the prediction of carbon and nitrogen in an Oxisol

Espectroscopia de reflectancia difusa por infrarrojo cercano (NIR) para la predicción de carbono y nitrógeno de un Oxisol

Jesús H. Camacho-Tamayo[1], Yolanda Rubiano S.[2], and Maria del Pilar Hurtado S.[3]

ABSTRACT

The characterization of soil properties through laboratory analysis is an essential part of the diagnosis of the potential use of lands and their fertility. Conventional chemical analyzes are expensive and time consuming, hampering the adoption of crop management technologies, such as precision agriculture. The aim of the present paper was to evaluate the potential of near-infrared (NIR) diffuse reflectance spectroscopy for the prediction of the carbon and nitrogen of Typic Hapludox. In the A and B horizons, 1,240 samples were collected in order to determine the total carbon (TC) and nitrogen (TN) contents, obtain the NIR spectral curve, and build models using partial least squares regression. The use of diffuse reflectance spectroscopy and statistical techniques allowed for the quantification of the TC with adequate models of prediction based on a small number of samples, an residual prediction deviation RPD greater than 2.0, an R^2 greater than 0.80 and a low root mean square error RMSE. For TN, models with a good level of prediction were not obtained. The results based on the NIR models were able to be integrated directly into the geostatistical evaluations, obtaining similar digital maps from the observed and predicted TC. The use of pedometric techniques showed promising results for these soils and constitutes a basis for the development of this area of research on soil science in Colombia.

Key words: Oxisol, pedometrics, soil mapping, geostatistics.

RESUMEN

La caracterización de las propiedades del suelo mediante análisis de laboratorio es parte esencial en el diagnóstico del potencial de uso de las tierras y de su fertilidad. Los análisis químicos convencionales son costosos y demorados, lo que dificulta la adopción de tecnologías de gestión de cultivos, como la agricultura de precisión. El objetivo del presente trabajo fue evaluar el potencial de la espectroscopía de reflectancia difusa por infrarrojo lejano (NIR) en la predicción del carbono y del nitrógeno de un Typic Hapludox. Se recolectaron 1.240 muestras en los horizontes A y B, para determinar los contenidos de carbono total (TC) y nitrógeno total (TN), obtener las respuestas espectrales NIR y elaborar los modelos mediante regresión por mínimos cuadrados parciales. El uso de las espectroscopía de reflectancia difusa y de técnicas estadísticas permitió la cuantificación del TC, con modelos de predicción adecuados con bajo número de muestras, desviación residual de la predicción RPD mayores de 2,0, R^2 mayores de 0,80 y error cuadrático medio RMSE bajos. Para TN no se obtuvieron modelos con buen nivel de predicción. Para TC, los resultados obtenidos a partir de los modelos NIR pudieron integrarse directamente en las evaluaciones geoestadísticas, obteniendo mapas digitales y espectro-digitales similares. El uso de las técnicas pedométricas, mostró resultados promisorios para estos suelos y se constituye en una base para el desarrollo de esta área de investigación de la ciencia del suelo en Colombia.

Palabras clave: Oxisol, pedometría, mapeo de suelos, geoestadística.

Introduction

The determination of characteristics and properties of soils through appropriate descriptions and laboratory analyses is a task that is basic to the understanding and evaluation of soil quality (Cortés and Malagón, 1984), where carrying out routine physical and chemical analyses is required, which in the majority of the cases are expensive and require time-consuming sample pre-processing or the use of (environmentally harmful) chemical extractants. This, along with some properties of the soil, principally the physical and chemical ones, which are not static and uniform in space and time, makes spatial and temporal analysis even more difficult because of the high number of samples required for a complete understanding of the dynamics of the soil (Plant, 2001).

Received for publication: 25 July, 2013. Accepted for publication: 19 March, 2014.

[1] Department of Civil and Agricultural Engineering, Faculty of Engineering, Universidad Nacional de Colombia. Bogota (Colombia). jhcamachot@unal.edu.co
[2] Department of Agronomy, Faculty of Agricultural Sciences, Universidad Nacional de Colombia. Bogota (Colombia).
[3] Environmental Laboratory Services, Centro Internacional de Agricultura Tropical (CIAT). Cali (Colombia).

There exists a worldwide search for the development of cheap and rapid methodologies for carrying out soil analyses (Shepherd and Walsh, 2007), which for example support environmental monitoring (Okin and Painter, 2004), modeling of biological or agricultural production processes in productive systems known as precision agriculture or site specific management (Cruz *et al*., 2011; Tittonell *et al*., 2008).

A technological option is the use of spectroscopy. Reflectance spectroscopy studies energy reflecting material as part of the division of the incident energy, depending on the wavelength. Various fractions of the energy incident on the element are reflected, absorbed, and or transmitted and occurs reflection specular and / or diffuse. Specular reflection occurs mainly on smooth (polished) surfaces, whose roughness is less than the considered wavelength. Diffuse reflection occurs especially on rough surfaces and is the result of the penetration of a portion of the incident beam to within the body, such as occurs with soil particles. In short, the energy reflected by a solid body is a combination of the two kinds of mentioned reflection and its magnitude depends on the particle size, structure, mineralogy and soil water content, microrelief, and other characteristics. For soils, visible and infrared spectra result from electronic and vibrational processes. Despite fundamental vibration bands that lie in the mid- and far-infrared regions, vibrational processes yield characteristics in the NIR region due to the excitation of overtones and combination of tones of the fundamental modes of anion groups (*e.g.,* OH, CO_3 and SO_4; Hunt and Salisbury, 1970). Therefore, soil constituents present weak, broad and, in most of the cases, over-lapping and masking VIS–NIR spectral responses. However, a soil VIS–NIR response contains important information about soil mineralogy.

Diffuse reflectance spectroscopy is a sensing method that can be utilized to enhance or replace conventional methods of soil analysis. This technique has undergone high development in the last two decades, overcoming some limitations and gaining a greater diversity of robust statistical methodologies that can more precisely relate the spectrum variability to the soil properties' variability. Soil spectroscopy is fast and convenient, less costly, non-destructive, simple, and, on occasion, more precise than conventional forms of analysis, reinforced by the use of other techniques such as multivariate statistics and geostatistics (Tittonel *et al*., 2008). The advantage of this technology is that a single spectrum allows for the simultaneous characterization of diverse soil properties.

The spectral band that extends from 1,000 to 2,500 nm (near infrared, NIR) is presently the most widely used in the observation of the spectral signature of soils. Commonly, air transported spectral sensors, as well as orbitals, cover the VIS and NIR bands. Although these bands are the ones most widely used, studies have also been carried out on the ultraviolet band (UV) (Bogrekci and Lee, 2007) or with the use of gamma rays (Elias, 2004; Pires *et al*., 2005).

The potential use of diffuse reflectance in agriculture and specifically in the study of soil properties has been employed by various authors (Cozzolino and Moron, 2006; Vasques *et al*., 2008; Sarkhot *et al*., 2011; Ramírez-Lopez *et al*., 2013), by means of the use of spectra in the VIS, NIR, and MIR regions. The absorption of energy in the visible (VIS) region and next to the near infrared (NIR) (between 400 and 1,500 nm) is due to the carbon content of the soil and to the iron oxides, especially through minerals such as hematite and goethite, while the NIR is strongly related to the water, clay minerals, carbonates and organic material content (Viscarra Rossel and Chen, 2011); seeing that, in the region of 2,200 and 2,300 nm, the kaolinite and gibbsite contents can be clearly identified. In the MIR region, by the same token, regions related to minerals and a great number of peaks, which are related to OH groups, can be defined, where the zone that spans 2,700 to 2,900 nm stands out. For these reasons, the aim of the present paper was to evaluate the potential of NIR diffuse reflectance spectroscopy for the prediction of carbon and nitrogen in Typic Hapludox from the eastern plains of Colombia and to later develop prediction maps with the spectral data models for carbon and nitrogen.

Materials and methods

Location and characterization of the area of study. This study was carried out at the Carimagua Experimental Station, located in the municipality of Puerto Gaitán (Meta, Colombia), with geographical coordinates 4°37'N and 71°19'W and an altitude of 175 m. The zone is characterized as having a slightly undulating relief, with slopes between 2 and 5%; covered with native savanna (used for more than 30 years for extensive cattle raising); and having a sub-humid tropical climate, with an average temperature of 27.8°C and average annual precipitation of 2,240 mm, which is concentrated between the months of April and November. The predominant soils of the zone are highly-fertilized Oxisols, which are characterized as being strongly acidic (pH <5) and having low organic matter contents. The studied soil belongs to the Carimagua-Tomo complex, with taxonomic components: Typic Hapludox and Tropectic Hapludox.

Field sampling and laboratory analysis. A system of rigid grid sampling was established, where containers were placed perpendicularly at 320 m, in an area of around 5,100 ha, totaling 470 profile points. In addition, 150 points were selected in a pilot area, equivalent to 10% of the area of study, in order to guarantee an observation of 2.5 ha. All of the points were georeferenced with GPS (precision ± 1 m) and the sampling of the soil was carried out for the surface A horizon and the subsurface B, for a total of 1,240 samples.

The samples were dried at a temperature of 35°C until they reached equilibrium moisture and sifted in a mesh of 2 mm for the determination of total carbon (TC) and total nitrogen (TN), using an element determinator (TruSpec CN Carbon Nitrogen Determinator, LECO, St. Joseph, MI). The spectral curves were acquired through a NIRS 6500 sensor (FOSS NIRSystems, Herisau, Switzerland), which gives a scan of spectral response at 2 nm, from an average of 64 scans per wavelength, in the region between 1,000 and 2,500 nm.

Data analysis. A qualitative characterization was carried out in which the intensity of the reflectance, the characteristic peaks, and the behavior at different depths were analyzed. Due to the heterogeneous composition of soils, the spectral curves hold information that is consisted of different combinations and overtones of spectral responses of the soil components, which results in a high number of representative bands, including simple compounds (Reeves III, 2010). According to Ramírez-López *et al.* (2013), the spectral responses of soils are non-specific, which makes the spectral information of soils highly complex. This makes the spectral curves of soils vary according to the concentration of the materials that compose them, allowing one to infer differences between soil samples, either for their classification or for the differentiation of horizons, even ending in proposing a classification of spectral curves, intimately related to characteristic peaks, principally given the mineral, organic material, iron oxide, sand, and clay content.

For the calibration of the models, 10 groups of 100, 200, 300, 400, 500, 600, 700, 800, 900, and 1,000 samples were formed, leaving 200 samples to validate the model obtained for each sample group. The formation of each group was done using the conditioned Latin Hypercube Sampling (cLHS) (Minasny and McBratney, 2006). The cLHS technique consists of selecting initial values for the construction of the model, stratifying the range of each one of the entry data of the model, in order to thus guarantee that the initial values of each range of the entry data are selected. This technique allows for the reduction of the number of simulations necessary to obtain a reasonable result.

In the calibrations, it was considered that the spectral responses could be normalized and could receive different mathematical treatment in order correct possible noise or deformities (preprocessing). Among these techniques, SNV (standard normal variation) was considered, with which inconvenient optics are corrected; along with detrend, in order to correct the tendency of the data; and MSC (multiplicative signal correction), which corrects the multiple dispersion and is recommended when various groups of samples are identified. It is also possible to smooth the points and eliminate some signal noise using various filters (*i.e.,* Median Filter, Wavelet, Savitzky-Golay).

For the elaboration of the models, the "leave one out" method was used, which provides information about the uncertainty of the models (generated with different partial least square –PLS- factors) based on the re-sampling method, from crossed validation. On the other hand, the number of PLS factors was chosen using the results of the validation of the models as a criterion, where the coefficient of determination (R^2), root mean square error (RMSE), mean error (ME), standard deviation error (SDE) and the residual prediction deviation (RPD) were considered. The calibration and validation of the models was done with the ParLes program v. 1.0, developed by Viscarra-Rosel (2008).

Once the models were calibrated and validated, the measurements of location and dispersion of the laboratory data (measured) and the predictions from the models were verified, where the similarity among the measured and predicted data could be observed. Afterwards, the experimental semivariograms were calculated, for the measured as well as for the predicted data from the models, with the established sample groups. Diverse theoretical models of semivariance exist, which can be fitted to the experimental semivariogram. Webster and Oliver (2007) presented a discussion with respect to the characteristics and conditions they should fulfill.

Once the model of best fit for each property was established, the degree of spatial dependence (DSD) was verified by means of the relation between the nugget effect and the sill. The DSD is classified as strong if it is higher than 75%, moderate for a DSD between 25 and 75%, and weak with a DSD below 25% (Cambardella *et al.*, 1994). It is important that the nugget effect not be greater than 50% of the value of the sill so that the model of spatial correlation can correctly describe reality (Cressie, 1993). In other situations, the noise in the measurements would explain the spatial

variability more than the correlation of the phenomenon. In these cases, the model fit to the experimental semivariogram is called the pure nugget effect (Goovaerts, 1998).

For the geostatistical analysis, GS^{+}™ v. 9 (Gamma Design Software, LLC, Plainwell, MI) was used, on the basis of which the theoretical semivariogram models were selected based on the least value of the sum of the squared residuals, the coefficient of determination (R^2) of the equation of fit and on the similar values obtained between the real value and the predicted value, which are obtained in the crossed validation (CVC), appropriate indicators for this purpose (Cucunubá-Melo *et al*., 2011).

Form the semivariogram models of the properties that expressed spatial dependency, the prediction was carried out by the ordinary kriging method, which is considered to be the best unbiased linear predictor, with minimum variance (Diggle and Ribeiro, 2000), for making a prediction at non-sampled sites, the results being presented by means of digital maps (with data obtained from laboratory data) and digital spectra (with data predicted from the models). This procedure was performed with the Surfer® program v.9 (Golden Software, Golden, CO).

Results and discussion

The spectral curves of soils from Carimagüa correspond to typical samples of Oxisols (Fig. 1), with low or medium contents of organic matter and the presence of iron oxides, but greater reflectances than those reported for Oxisols in Sao Paulo (Brazil) by Demattê *et al.* (2012) and Genú and Demattê (2012) and for Oxisols in Hawaii (USA) by McDowell *et al.* (2012), indicating a greater effect from the processes of weathering on the Eastern Plains of Colombian, associated with a higher average annual temperature and greater precipitation. The growing behavior of between 1,000 and 1,300 nm allows for the confirmation that they are highly weathered soils (Demattê *et al*., 2004). In these curves, the high contents of kaolinite in the clay can be verified, which are manifested in the peaks located at 1,900 and 2,200 nm, for all sites and horizons (Genú and Demattê, 2012). In a similar manner, the presence of gibbsite can be verified through the slight concavity that is exhibited at 2,265 nm.

The small reflectance at the beginning of the curves (1,000-1,400 nm) is directly related to the contents of TC (or organic material) and greater contents of Fe_2O_3 present in the goethite (Demattê *et al*., 2004). In general, organic material absorbs energy and promotes a low intensity of reflectance throughout the spectrum, which tends to diminish at greater wavelengths, which is also exhibited in the subsurface horizons (McDowell *et al*., 2012). Because of this, it can be observed that the curves of the analyzed subsurface horizons show greater reflectance, due to the smaller content of TC as well as iron, which is manifested principally at the beginning and the middle of the curves.

The results of the elaboration of the models can be seen in Tab. 1, which correspond to the calibration of the models for each group of samples and the validation of them with 200 samples. For the construction of the models, around 100 fits were tried for each property, resulting from the combination of transformations or the application of pre-processing, pre-treatments, derivation, or elimination of noise in the spectral curves. Of these models, those that showed the least RMSE and the greatest values of R^2 and RPD were used.

For TC, a more robust model was obtained than for TN, as can be observed in the results for the models of calibration and validation (Tab. 1), with an R^2 greater than 0.70 in the calibration as well as in the validation of the model. Various

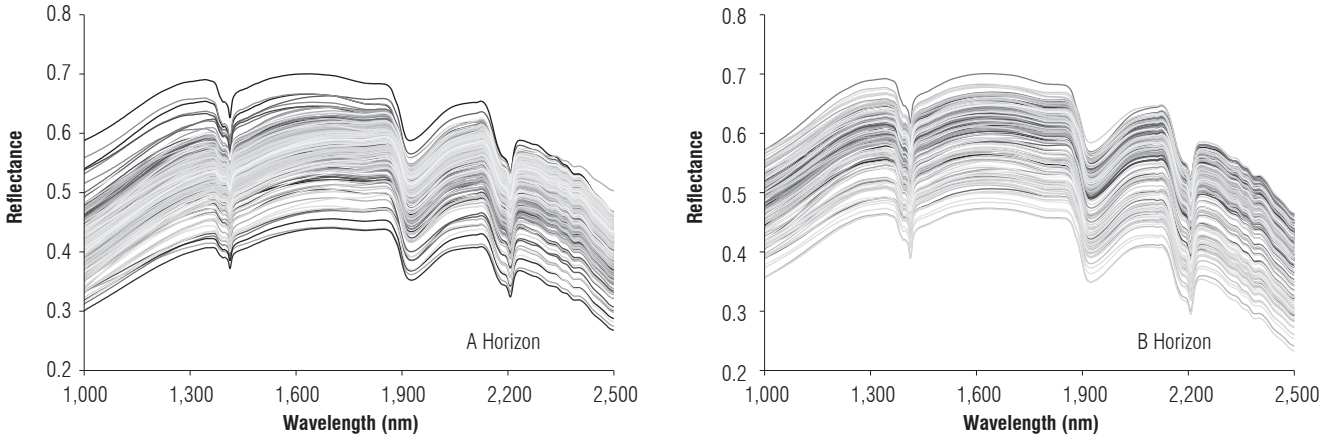

FIGURE 1. Spectral curves of the Oxisol from the Carimagua Experimental Station (Puerto Gaitán, Colombia) for the A (left) and B (right) horizons.

TABLE 1. Results of the calibration and validation of the models for total carbon (TC) and total nitrogen (TN).

Samples	TC calibration			TC validation			TN calibration			TN validation		
	R^2	RMSE	RPD	R^2	RMSE	RPD	R^2	RMSE	RPD	R^2	RMSE	RPD
100	0.77	0.26	2.09	0.74	0.28	2.02	0.20	0.04	1.12	0.23	0.03	1.17
200	0.79	0.25	2.17	0.77	0.26	2.13	0.25	0.03	1.15	0.25	0.03	1.19
300	0.81	0.24	2.27	0.80	0.24	2.08	0.28	0.03	1.18	0.27	0.03	1.22
400	0.83	0.22	2.43	0.82	0.23	2.18	0.31	0.03	1.20	0.30	0.03	1.24
500	0.85	0.21	2.58	0.83	0.22	2.22	0.35	0.03	1.24	0.32	0.03	1.24
600	0.86	0.20	2.67	0.85	0.21	2.21	0.38	0.03	1.27	0.36	0.03	1.25
700	0.87	0.19	2.80	0.86	0.20	2.24	0.39	0.03	1.28	0.37	0.03	1.24
800	0.87	0.19	2.91	0.87	0.20	2.26	0.42	0.03	1.31	0.38	0.03	1.25
900	0.88	0.19	2.95	0.87	0.19	2.27	0.43	0.03	1.33	0.39	0.03	1.26
1,000	0.89	0.18	2.99	0.88	0.19	2.27	0.44	0.03	1.33	0.42	0.03	1.26

R^2, coefficient of determination; RPD, residual prediction deviation; RMSE, root mean square error.

forms of carbon, either organic, total, or the fractions that it is composed of, exhibit good models regardless of the soil class that is studied (Vasques *et al*., 2008; Sarkhot *et al*., 2011; McDowell *et al*., 2012; Kodaira and Shibusawa, 2013).

For the calibrations carried out for the 10 groups defined for each property with the representative models, it was verified that when the number of samples increased, the values of the R^2 and the RPD increased, while the RMSE diminished, showing that an increase in the samples allows for the creation of more robust models.

It must also be considered that the RMSE, which depends on the studied property, was low. In general, these values vary according to the soil class and the quantity that a specific element can exhibit. For the present study, the values of RMSE found for TC and TN were close to or less than those reported in different soil classes by other authors (Gogé *et al*., 2012). In a similar manner, the RMSE varied sensitively when a low number of samples was used, independent of the property, which justifies not using a low number of samples for the construction of the models.

On the other hand, the residual prediction deviation (RPD) is the factor that indicates the precision behavior of the prediction in comparison with the average composition of all the samples. For this factor, Saeys *et al.* (2005) stated that models with an RPD less than 1.5 indicate that the calibration cannot be used, values of RPD between 1.5 and 2.0 reveal the possibility of differentiating the variability of the data, while values of RPD greater than 2.0 indicate a better predictive performance of the model; RPDs greater than 3.0 are considered excellent. Without a doubt, the interpretation of the value of the RPD depends on the context and the purpose for which the measurements and predictions will be used (Fearn, 2002), especially when one works with heterogeneous materials such as soil. In general, various authors prefer to work with RPDs obtained in the validation, where RPDs< 1.4 are considered slightly or not at all representative, values of RPD between 1.4 and 2.0 are considered for reasonable predictions, and RPDs > 2.0 are considered excellent for prediction (Chang *et al*., 2001; Cozzolino and Moron, 2006; Minasny *et al*., 2009; Kodaira and Shibusawa, 2013), from which it is emphasized that the resultant model for TN does not show an adequate level of predictability.

Once the models were calibrated and validated, measures of location and dispersion on the laboratory data (measured) and those predicted from the models were verified (Tab. 2),

TABLE 2. Descriptive statistics of the contents of total carbon (TC) and total nitrogen (TN) for the measured (Mea) and predicted (Pre) data from the spectral models.

Property	Mean	Median	cv (%)	Minimum	Maximum	Skewness	Curtosis
				A horizon			
TC_{Mea}	1.884	1.890	13.70	1.190	2.550	-0.03	-0.09
TC_{Pre}	1.888	1.899	11.19	1.136	2.422	-0.20	-0.03
TN_{Mea}	0.122	0.121	25.94	0.033	0.212	0.19	0.09
TN_{Pre}	0.119	0.118	13.87	0.076	0.174	0.42	0.51
				B horizon			
TC_{Mea}	0.917	0.920	21.51	0.351	1.550	0.26	0.20
TC_{Pre}	0.945	0.952	21.91	0.332	1.526	0.01	-0.10
TN_{Mea}	0.071	0.069	33.26	0.009	0.153	0.35	0.12
TN_{Pre}	0.072	0.073	15.83	0.036	0.113	-0.21	0.26

cv, coefficient of variation.

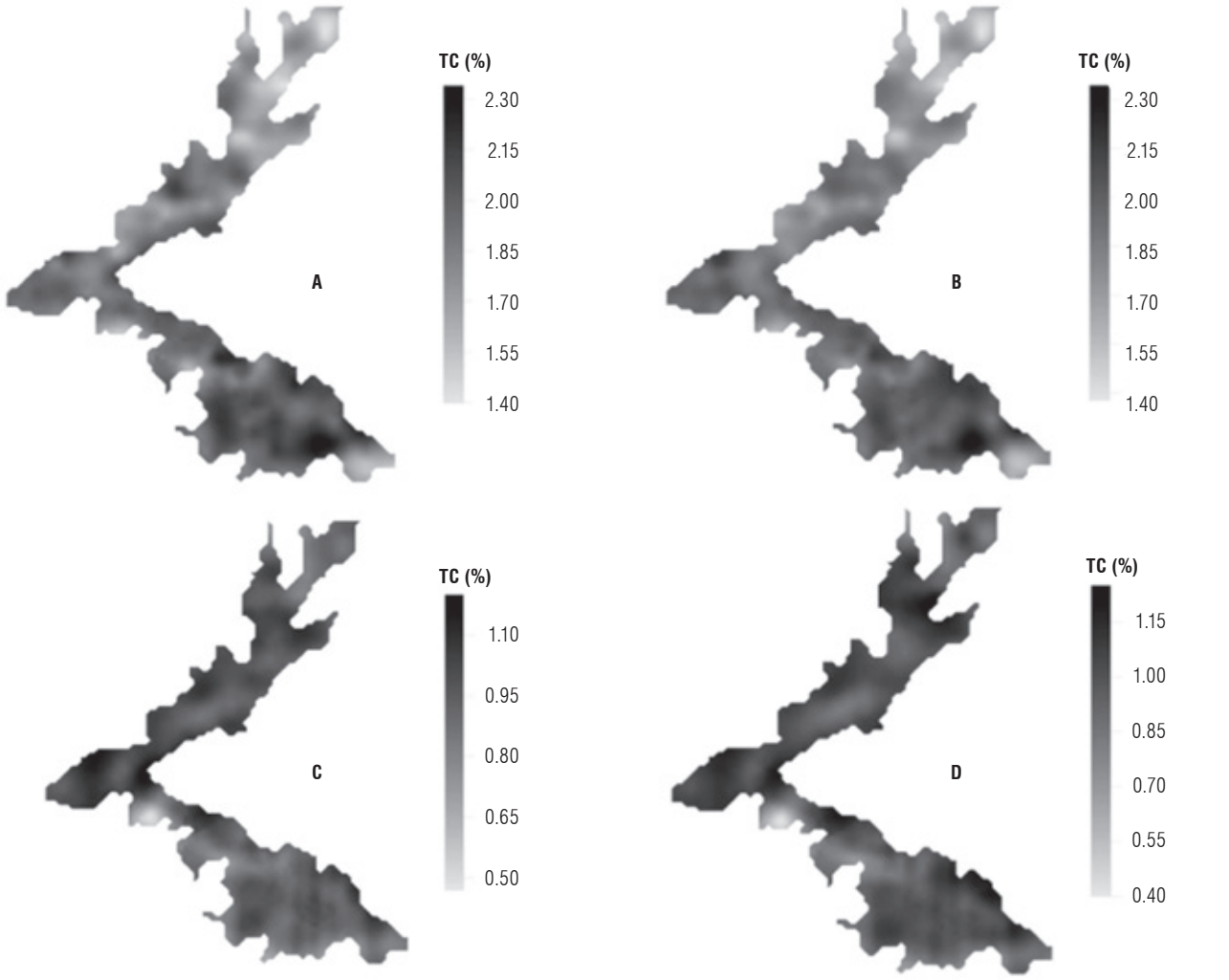

FIGURE 2. Contour maps of total carbon-TC for the A horizon (A, measured and B, predicted) and for the B horizon (C, measured and D, predicted).

TABLE 3. Parameters of the theoretical semivariogram models, obtained for total carbon and total nitrogen for measured and predicted data from spectral models.

Parameters	Total carbon (%)		Total nitrogen (%)	
	Measured	Predicted	Measured	Predicted
		A horizon		
Model	Spherical	Spherical	Exponential	Exponential
C_0	0.033	0.017	$1.07 \cdot 10^{-4}$	$3.21 \cdot 10^{-5}$
$C_0 + C$	0.067	0.041	$9.34 \cdot 10^{-4}$	$3.09 \cdot 10^{-4}$
Range. m	1120	1250	870	960
R^2	0.80	0.76	0.75	0.73
CVC	0.86	0.91	0.74	0.90
DSD	0.51	0.58	0.89	0.82
		B horizon		
Model	Spherical	Spherical	Exponential	Exponential
C_0	0.023	0.021	$5.5 \cdot 10^{-5}$	$3.7 \cdot 10^{-5}$
$C_0 + C$	0.048	0.041	$4.5 \cdot 10^{-4}$	$1.4 \cdot 10^{-4}$
Alcance. m	2100	2040	660	3450
R^2	0.91	0.93	0.67	0.94
CVC	0.90	0.95	0.67	0.95
DSD	0.50	0.53	0.92	0.59

CVC: cross validation coefficient; DSD: degree of spatial dependence

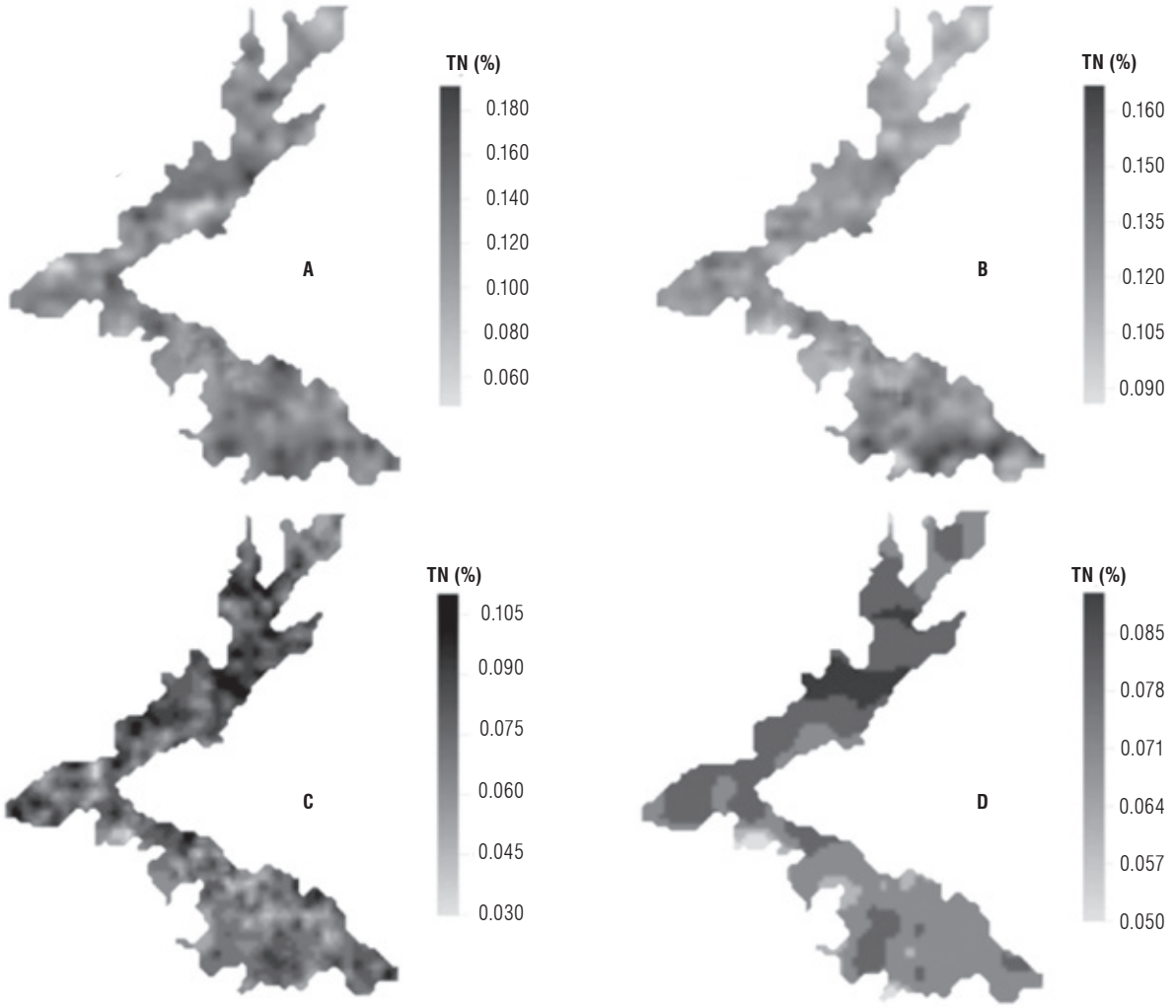

FIGURE 3. Contour maps of total nitrogen-TN for the A horizon (A, measured and B, predicted) and for the B horizon (C, measured and D, predicted).

where the similarity between the measured data and the predicted data can be observed. This similarity is greater for TC, due to the better performance of the model with respect to the results obtained for TN, with similar values of mean and median, as well as of the behavior of the coefficient of variation (CV) and the skewness and kurtosis. The low representatively found for the nitrogen model is verified by the greater difference in the CV between the minimum and maximum values, as well as between the measured and predicted values.

The contents of TC varied between low and medium, the content in the A horizon was greater due to the presence of vegetation and residues at the surface. The TN showed a behavior similar to the TC. The values found in this study coincide with those reported by Phiri *et al.* (2001) and Camacho-Tamayo *et al.* (2008).

On the other hand, the spatial behavior of TC and TN was analyzed from the measured and predicted data (Tab. 3). Large differences between the measured and predicted data were not observed from the spectral models. In general, the use of predicted data in the construction of semivariograms does not modify the tendency of spatial variation of the properties, as is verified in the obtained models, although differences for TN in the B horizon were identified due to the poor representativity of the model. For the other results, values of R^2 and CVC above 0.70 can be observed, with a similar range and DSD.

It is convenient to point out that the spatial variability of the soil properties and their relation to the errors associated with the sampling can promote changes in the results. On the other hand, errors in the soil sampling are generally greater than the errors derived from the soil analysis in particular (Cantarella *et al.*, 2006). This gives a large advantage to the use of reflectance spectroscopy since its outliers can be rapidly and efficiently identified before the laboratory analysis, when models are elaborated, allowing

a savings of time and economic resources in samples that possibly do not give information that is relevant or related to the aim of a specific study.

With the results obtained in the semivariogram models, contour maps were constructed for TC (Fig. 2) and TN (Fig. 3), on the basis of ordinary kriging. The contour maps obtained for the TC from the predicted data (spectral maps) showed a high correspondence with the maps obtained from measured values for each horizon, with coefficients of determination above 0.85 for the two horizons studied. For TN, the map obtained from the laboratory data differs from the spectral map, given that the prediction of the data from the model obtained is not adequate.

The results confirm that the prediction made for TC from the spectral models in the NIR regions is an effective tool, which together with computational and statistical techniques, provides the basis of high-resolution field scale mapping of TC, through source reliable information. These results enable its applicability in geologically homogeneous areas, which, in the case of Colombia, cover about 20 million hectares (Phiri *et al*., 2001) in the Eastern Plains, an area that has had high agricultural development in the last decade.

Conclusions

The coefficient of correlation found in the calibration and validation of the model of TC, together with the low amount of errors found, indicates that laboratory analyses can substitute, in large part, for spectral models. In the case of TN, it would be convenient to improve the model so that, in the future, laboratory analyses can be substituted.

The use of predicted values of soil properties from spectral models allows for the identification of the spatial structures of the properties; that is to say, this methodology can be implemented in the mapping of the spatial variability of soil properties.

Literature cited

Bogrekci, I. and W.S. Lee. 2007. Comparison of ultraviolet, visible, and near infrared sensing for soil phosphorus. Biosyst. Eng. 96(2), 293-299.

Chang, C.W., D.A. Laird, M.J. Mausbach, and C.R. Hurburgh Jr. 2001.Near-infrared reflectance spectroscopy-principal components regression analysis of soil properties. Soil Sci. Soc. Amer. J. 65(2), 480-490.

Camacho-Tamayo, J.H., C.A. Luengas, and F.R. Leiva. 2008. Effect of agricultural intervention on the spatial variability of some soils chemical properties in the eastern plains of Colombia. Chilean J. Agric. Res. 68(1), 42-55.

Cambardella, C.A., T.B. Moorman, J.M. Novak, T.B. Parkin, D.L. Karlen, R.F. Turco, and A.E. Konopka. 1994. Field-scale variability of soil properties in Central Iowa Soils. Soil Sci. Soc. Am. J. 58(5), 1501-1511.

Cantarella, H., J.A. Quaggio, B. Van Raij, and M.F. Abreu. 2006. Variability of soil analysis in commercial laboratories: implications for lime and fertilizer recommendations. Comm. Soil Sci. Plant Anal. 37, 2213-2225.

Cortés L., A. and D. Malagón C. 1984. Los levantamientos agrológicos y sus aplicaciones múltiples. Universidad Jorge Tadeo Lozano, Bogota.

Cozzolino, D. and A. Morón. 2006. Potential of near-infrared reflectance spectroscopy and chemometrics to predict soil organic carbon fractions. Soil Till. Res. 85(1-2), 78-85.

Cressie, N. 1993. Statistics for spatial data. John Wiley & Sons, New York, NY.

Cruz, J.S. R.N. Assis Júnior, S.S.R. Matías, and J.H. Camacho-Tamayo. 2011. Spatial variability of an Alfisol cultivated with sugarcane. Cien. Inv. Agr. 38, 155-164.

Cucunubá-Melo, J.L., J.G. Álvarez Herrera, and J.H. Camacho-Tamayo. 2011. Identification of agronomic management units based on physical attributes of soil. J. Soil Sci. Plant Nutr. 11(1), 87-99.

Demattê, J.A.M., R.C. Campos, M.C. Alves, P.R. Fiorio, and M.R. Nanni. 2004. Visible–NIR reflectance: a new approach on soil evaluation. Geoderma 121(1-2), 95-112.

Demattê, J.A.M., F.S. Terra, and C.F. Quartaroli. 2012. Spectral behavior of some modal soil profiles from São Paulo State, Brazil. Bragantia 71(3), 413-423.

Diggle, P. and J. Ribeiro. 2000. Model based geostatistics. Associação Brasileira de Estatística, São Paulo, Brazil.

Elias, A.E. 2004. A simplified analytical procedure for soil particle-size analysis by gamma-ray attenuation. Comput. Electron. Agric. 42(3), 181-184.

Fearn, T. 2002. Assessing calibrations: SEP, RPD, RER and R^2. NIR News 13(6), 12-14.

Genú, A.M. and J.A.M. Dematte. 2012. Espectrorradiometria de solos e comparação com sensores orbitais. Bragantia 71(1), 82-89.

Gogé, F., R. Joffre, C. Jolivet, I. Ross, and L. Ranjard. 2012.Optimization criteria in sample selection step of local regression for quantitative analysis of large soil NIRS database. Chemometr. Intell. Lab. Syst. 110(1), 168-176.

Goovaerts, P. 1998. Geostatistical tools for characterizing the spatial variability of microbiological and physico-chemical soil properties. Biol. Fertil. Soils 27(4), 315-334.

Hunt, G.R. and J.W. Salisbury. 1970. Visible and near infrared spectra of minerals and rocks. I. Silicateminerals. Mod. Geol. 1, 283-300.

Kodaira, M. and S. Shibusawa. 2013. Using a mobile real-time soil visible-near infrared sensor for high resolution soil property mapping. Geoderma 199, 64-79.

McDowell, M.L., G.L. Bruland, J.L. Deenik, S. Grunwald, and N.M. Knox. 2012. Soil total carbon analysis in Hawaiian soils with visible, near-infrared and mid-infrared diffuse reflectance spectroscopy. Geoderma 189-190, 312-320.

Minasny, B. and A.B. McBratney. 2006. A conditioned latin hypercube method for sampling in the presence of ancillary information. Comput. Geosci. 32(9), 1378-1388.

Minasny, B., G. Tranter, A.B. McBratney, D.M. Brough, and B.W. Murphy. 2009. Regional transferability of mid-infrared diffuse reflectance spectroscopic prediction for soil chemical properties. Geoderma 153(1-2), 155-162.

Okin, G.S. and T.H. Painter. 2004. Effect of grain size on remotely sensed spectral reflectance of sandy desert surfaces. Rem. Sens. Environ. 89(3), 272-280.

Phiri, S., E. Amézquita, I.M. Rao, and B.R. Singh. 2001. Disc harrowing intensity and its impact on soil properties and plant growth of agropastoral systems in the Llanos of Colombia. Soil Till. Res. 62(3-4), 131-143.

Pires, L.F., O.O.S. Bacchi, and K. Reichardt. 2005. Soil water retention curve determined by gamma-ray beam attenuation. Soil Till. Res. 82(1), 89-97.

Plant, R. 2001. Site-specific management: The application of information technology to crop production. Comput. Electron. Agric. 30(1-3), 9-29.

Ramírez-Lopez, L., T. Behrens, K. Schmidt, R. Viscarra Rossel, J.A.M. Demattê, and T. Scholten. 2013. The spectrum-based learner: A new local approach for modeling soil vis–NIR spectra of complex datasets. Geoderma 195-196, 268-279.

Reeves III, J.B. 2010. Near- versus mid-infrared diffuse reflectance spectroscopy for soil analysis emphasizing carbon and laboratory versus on-site analysis: Where are we and what needs to be done? Geoderma 158(1-2), 3-14.

Saeys, W., A.M. Mouazen, and H. Ramon. 2005. Potential for onsite and online analysis of pig manure using visible and near infrared reflectance spectroscopy. Biosyst. Eng. 91(4), 393-402.

Sarkhot, D.V., S. Grunwald, Y. Ge, and C.L.S. Morgan. 2011. Comparison and detection of total and available soil carbon fractions using visible/near infrared diffuse reflectance spectroscopy. Geoderma 164(1-2), 22-32.

Shepherd, K. and M. Walsh. 2007. Infrared spectroscopy - enabling an evidence based diagnostic surveillance approach to agricultural and environmental management in developing countries. J. Near Infrared Spectrosc. 15(1), 1-19.

Tittonell, P., K. Shepherd, B. Vanlauwe, and K. Giller. 2008. Unravelling the effects of soil and crop management on maize productivity in smallholder agricultural systems of western Kenya: An application of classification and regression tree analysis. Agric. Ecosyst. Environ. 123(1-3), 137-150.

Vasques, G.M., S. Grunwald, and J.O. Sickman. 2008. Comparison of multi-variate methods to predict soil carbon using visible/near-infrared diffuse reflectance spectroscopy. Geoderma 146(1-2), 14-25.

Viscarra Rossel, R.A. 2008. ParLeS: Software for chemometric analysis of spectroscopic data. Chemometr. Intell. Lab. Syst, 90(1), 72-83.

Viscarra Rossel, R.A. and C. Chen. 2011. Digitally mapping the information contente of visible-near infrared spectra of surficial Australian soils. Rem. Sens. Environ. 115(6), 1443-1455.

Webster, R. and M.A. Oliver. 2007. Geostatistics for environmental scientists. John Wiley & Sons, Hoboken, NJ.